Matching Structures by Computing Minimal Paths on a Manifold

Etienne Huot, Hussein Yahia, Isaac Cohen, Isabelle Herlin

▶ **To cite this version:**

Etienne Huot, Hussein Yahia, Isaac Cohen, Isabelle Herlin. Matching Structures by Computing Minimal Paths on a Manifold. Journal of Visual Communication and Image Representation, 2002, 13 (1), pp.302-312. 10.1006/jvci.2001.0485 . hal-00948350

HAL Id: hal-00948350

https://inria.hal.science/hal-00948350

Submitted on 18 Feb 2014

HAL is a multi-disciplinary open access archive for the deposit and dissemination of scientific research documents, whether they are published or not. The documents may come from teaching and research institutions in France or abroad, or from public or private research centers.

L'archive ouverte pluridisciplinaire **HAL**, est destinée au dépôt et à la diffusion de documents scientifiques de niveau recherche, publiés ou non, émanant des établissements d'enseignement et de recherche français ou étrangers, des laboratoires publics ou privés.

Journal of Visual Communication and Image Representation **13**, 302–312 (2002)
doi:10.1006/jvci.2001.0485, available online at http://www.idealibrary.com on IDEAL®

SHORT COMMUNICATION

Matching Structures by Computing Minimal Paths on a Manifold

Etienne Huot and Hussein Yahia

INRIA, Air Project, Domaine de Voluceau - B.P. 105, 78153 Le Chesnay Cedex, France
E-mail: Etienne.Huot@inria.fr, Hussein.Yahia@inria.fr

Isaac Cohen

IRIS, University of Southern California, Powell Hall, PHE218, Los Angeles, California 90089-0273
E-mail: icohen@iris.usc.edu

and

Isabelle Herlin

INRIA, Air Project, Domaine de Voluceau - B.P. 105, 78153 Le Chesnay Cedex, France
E-mail: Isabelle.Herlin@inria.fr

Received February 7, 2000; accepted June 25, 2000

The general problem of matching structures is very pervasive in computer vision and image processing. The research presented here tackles the problem of object matching in a very general perspective. It is formulated for the matching of surfaces. It applies to objects having small or large deformation and arbitrary topological changes. The process described hinges on a geodesic distance equation for a family of curves or surfaces embedded in the graph of a cost function. This geometrical approach to object matching has the advantage that the similarity criterion can be used to define the shape of the cost function. Matching paths are computed on the cost manifolds using distance maps. These distance maps are generated by solving a general partial differential equation which is a generalization of the geodesic distance evolution scheme introduced by R. Kimmel, A. Amir, and A. F. Bruckstein (1995, *IEEE Trans. Pattern Anal. Mach. Intell.* **17**, 635–640). An Eulerian level-set formulation is also introduced, leading to a numerical scheme used for solving partial differential equations originating from hyperbolic conservation laws, which has proven to be very robust and stable. © 2002 Elsevier Science (USA)

1047-3203/02 $35.00
© 2002 Elsevier Science (USA)
All rights reserved.

1. INTRODUCTION AND PREVIOUS WORKS

Matching structures is a major area for image processing and it involves a lot of classical applications such as stereo vision, temporal tracking, and matching of different acquisitions. The characterization of a matching function is an ill-posed problem in the sense that there is no unique solution. However, introducing structures properties such as their geometry or the underlying image representation allows the characterization of a unique matching function. Commonly used features are pixel gray level values for stereoscopic matching or optical flow [6], edges for token based approaches [23], and geometric properties of the structures [24, 25]. The latter properties are more robust since they can deal with situations where there is no consistency of image gray level. Relevant geometrical properties are selected on the basis of their ability to characterize a description of the structures which is invariant to the considered deformation. In the case of rigid or small elastic deformations high curvature points [4, 16] or semi-differential invariants [22] can be considered as an invariant description of the structure. Higher order geometric description such as crest and ridge lines can also be considered in order to characterize volume structures properties [20, 21]. Such methods perform well in the case of small deformation but cannot deal with large deformation and topological change. Such problems occur when we are interested in studying the evolution of a structure whose topology evolves in time [5].

In this paper we present a generalization to higher dimensions of a curve matching process described in [5], and we also generalize a curve evolution process introduced by Kimmel *et al.* [12]. Curve evolution methods are becoming increasingly used in computer vision. Classical work of Kass *et al.* [11] has been reformulated in the context of PDE-driven curves and surfaces (Malladi *et al.* [13], Caselles *et al.* [3], Gomes *et al.* [9] *etc.*). In this work a new normal surface evolution is used to deduce a surface matching process.

The extension of the classical curve evolution process is presented in Section 2. The definition of the geodesic distance evolution equation is presented in Section 2.1. Sections 2.1.1 to 2.1.3 present the problem, introduce the Hodge operator, and introduce the evolution equation. Section 2.1.4 is devoted to deriving the equation of the projection, while Section 2.1.5 presents the level-set formulation. A surface matching is then deduced and described in Section 2.2. Section 2.3 presents a result related to meteorological data.

2. SURFACE MATCHING

This section addresses the problem of surface matching. The method proposed is based on a generalization of the algorithm introduced by Cohen *et al.* in [5] for curves. This scheme has also motivated a generalization of the geodesic curve propagation method [12] into a surface evolution framework that is used for deriving a cost hypersurface $W \subset \mathbb{R}^4$ measuring the similarity of the surfaces to be matched. We begin by setting up a geodesic distance evolution scheme for evolving surfaces.

2.1. Geodesic Distance

2.1.1. A geodesic distance evolution rule for propagating surfaces on a 3-manifold. Let X be a 3-manifold (or hypersurface) in $\mathbb{R}^4$. We suppose X compact and pathwise connected.[1]

[1] These assumptions do not restrict the validity of the theory presented in this work, as the manifold X will appear as the graph of a cost function, which automatically satisfies these requiremenrs in practice.

From these assumptions, one can derive, using an easy application of the Hopf–Rinow–De Rham Theorem (see [19]) that given any two points M_0 and $M_1 \in X$, there exists a path $\gamma : [0, 1] \to X$ connecting M_0 and M_1 ($\gamma(0) = M_0,\ \gamma(1) = M_1$) whose length minimizes the lengths of all paths between the two points. The length of γ is called the geodesic distance between M_0 and M_1 and will be denoted $d_X(M_0, M_1)$ in the remainder of the paper. Moreover, the path γ is necessarily a geodesic curve on X, i.e., a curve such that the second derivative $\mathrm{d}^2\gamma/\mathrm{d}u^2$ is always perpendicular to X (Where u is the arclength of γ). Let $\mathcal{Y} \subset X$ be a surface (2-manifold) "drawn" on X. We consider the surfaces $\Xi_t \subset X$ whose points are located at geodesic distance t from $\mathcal{Y}$:

$$\Xi_t = \{M \in X \mid d_X(M, \mathcal{Y}) = t\}. \tag{1}$$

We are interested in defining a partial differential equation governing the evolution of the surface Ξ_t as the parameter t evolves. For this purpose, we will need a notion of cross-product in 4-space and a method of deriving simple formulae about such a cross-product. These formulae are needed in the demonstration of intermediate propositions. One mathematical tool that can achieve these requirements is given by the Hodge $*$ operator, a notion recalled in the next section.

2.1.2. Exterior algebras and the hodge $*$ operator. The theory is only briefly reviewed here. The reader is referred to [1] for a complete presentation of the subject. Let $\Lambda^p(\mathbb{R}^n)$ be the p-exterior power of space $\mathbb{R}^n$ and $*$ the Hodge operator defined, for every $\lambda \in \Lambda^p(\mathbb{R}^n)$ by the equality:

$$\lambda \wedge \mu = \langle *\lambda, \mu \rangle_{n-p} e_1 \wedge e_2 \wedge \cdots \wedge e_n. \tag{2}$$

In Eq. (2) $(e_1, \ldots, e_n)$ is the standard basis of $\mathbb{R}^n$, $\langle , \rangle_p$ is the usual dot product on $\Lambda^p(\mathbb{R}^n)$ defined on generators by

$$\langle u_1 \wedge \cdots \wedge u_p, w_1 \wedge \cdots \wedge w_p \rangle_p = \det(\langle u_i, w_j \rangle), \tag{3}$$

and $\mu \in \Lambda^{n-p}(\mathbb{R}^n)$. From the property $*(*\lambda) = (-1)^{p(n-p)}\lambda$, one can deduce that, if u, v, and w are three linearly independent vectors in $\mathbb{R}^4$, the associated image $*(u \wedge v \wedge w) \in \Lambda^1(\mathbb{R}^4) = \mathbb{R}^4$ satisfies the following properties:

- it is a vector in $\mathbb{R}^4$ perpendicular to u, v, and w.
- The basis $(u, v, w, *(u \wedge v \wedge w))$ is positively oriented.
- Its squared norm: $\|*(u \wedge v \wedge w)\|^2$ is equal to $\begin{vmatrix} \langle u, u \rangle & \langle u, v \rangle & \langle u, w \rangle \\ \langle v, u \rangle & \langle v, v \rangle & \langle v, w \rangle \\ \langle w, u \rangle & \langle w, v \rangle & \langle w, w \rangle \end{vmatrix}$.

Using the Hodge $*$ operator, we will derive the geodesic distance evolution scheme for the family of surfaces $\alpha(u, v, t)$. This is presented in the following section.

2.1.3. The geodesic distance evolution equation. We will make use of the following fact, proved in [7, p. 183]:

LEMMA 2.1. *Around any point on a surface one can always find a local orthogonal parameterization.*

So let $\alpha(u, v, t)$ be a local orthogonal parameterization of a family of surfaces in X, and let $\boldsymbol{\tau}^{\mathbf{u}} = \alpha_u/\|\alpha_u\|$, $\boldsymbol{\tau}^{\mathbf{v}} = \alpha_v/\|\alpha_v\|$ denote the two unitary tangent vectors determined by α

and $\mathbf{N}$ the normal vector to X. We suppose that the family $\alpha(u, v, t)$ satisfies the following partial differential equation:

$$\frac{\partial \alpha}{\partial t} = *(\mathbf{N} \wedge \boldsymbol{\tau}^{\mathbf{u}} \wedge \boldsymbol{\tau}^{\mathbf{v}}). \tag{4}$$

We want to prove that, for each t, $\alpha(u, v, t)$ is a local parameterization of Ξ_t. Let $\beta(t)$ be the curve in X defined by $\beta(t) = \alpha(u, v, t)|_{u=u_0, v=v_0, \text{fixed}}$. Then:

LEMMA 2.2. *For any u_0, v_0, the curve $\beta(t)$ is a geodesic in X.*

Proof. We prove this lemma by showing that β_{tt} is perpendicular to $\boldsymbol{\tau}^{\mathbf{u}}$, $\boldsymbol{\tau}^{\mathbf{v}}$, and $*(\mathbf{N} \wedge \boldsymbol{\tau}^{\mathbf{u}} \wedge \boldsymbol{\tau}^{\mathbf{v}})$. The only possibility that will remain will be that β_{tt} is collinear to $\mathbf{N}$ which means that β is a geodesic (by definition).

First note that

$$\beta_t = \frac{d\beta}{dt} = \frac{\partial \alpha}{\partial t} = *(\mathbf{N} \wedge \boldsymbol{\tau}^{\mathbf{u}} \wedge \boldsymbol{\tau}^{\mathbf{v}}),$$

so

$$\|\beta_t\|^2 = \left\| *(\mathbf{N} \wedge \boldsymbol{\tau}^{\mathbf{u}} \wedge \boldsymbol{\tau}^{\mathbf{v}}) \right\|^2 = 1 - \langle \mathbf{N}, \boldsymbol{\tau}^{\mathbf{u}} \rangle^2 - \langle \mathbf{N}, \boldsymbol{\tau}^{\mathbf{v}} \rangle^2 = 1$$

since the parameterization is orthogonal. This proves:

$$\langle \beta_{tt}, \beta_t \rangle = \left\langle \frac{d^2\beta}{dt^2}, \frac{d\beta}{dt} \right\rangle = \left\langle \frac{d}{dt}(*(\mathbf{N} \wedge \boldsymbol{\tau}^{\mathbf{u}} \wedge \boldsymbol{\tau}^{\mathbf{v}})), *(\mathbf{N} \wedge \boldsymbol{\tau}^{\mathbf{u}} \wedge \boldsymbol{\tau}^{\mathbf{v}}) \right\rangle = 0. \tag{5}$$

Hence, β_{tt} is perpendicular to $*(\mathbf{N} \wedge \boldsymbol{\tau}^{\mathbf{u}} \wedge \boldsymbol{\tau}^{\mathbf{v}})$.

Now, using methods similar to the one used in the 2D case (see proof of Lemma 1 in [12]), one can show that

$$\langle \beta_{tt}, \boldsymbol{\tau}^{\mathbf{u}} \rangle = 0, \text{ and similarly } \langle \beta_{tt}, \boldsymbol{\tau}^{\mathbf{v}} \rangle = 0. \tag{6}$$

The curve $\beta(t)$ is a geodesic in X. ■

LEMMA 2.3. *The evolution of the family of surfaces Ξ_t is given by the equation*

$$\frac{\partial \alpha}{\partial t} = *(\mathbf{N} \wedge \boldsymbol{\tau}^{\mathbf{u}} \wedge \boldsymbol{\tau}^{\mathbf{v}}). \tag{7}$$

The proof of this lemma is not given here, as it is a simple adaptation, using the the general Gauss lemma [19] of the proof given in [12, Lemma 2].

The two preceding lemmas demonstrate that, using the Hodge $*$ operator, it is possible to derive a geodesic distance evolution scheme for a family of surfaces described by local orthogonal parameterizations. In the next section, we compute the normal speed of the projection of Ξ_t onto the (x, y, z) hyperplain in $\mathbb{R}^4$.

2.1.4. Geodesic distance computation. Equation (7) cannot be solved directly in a general context. We follow the method described in (12) by considering the evolution of the projection. We now make the assumption that X is a graph hypersurface W, that is to say $X = W = \{(x, y, z, w(x, y, z))\}$ for a function $w : \mathbb{R}^3 \to \mathbb{R}$. Let $\pi : \mathbb{R}^4 \to \mathbb{R}^3$ be the

canonical projection onto the (x, y, z) hyperplan in $\mathbb{R}^4$ and let $S(t)$ be the projection of the image of $\alpha(u, v, t)$ (that is to say, Ξ_t) onto that hyperplan:

$$\mathcal{C}(t) = \pi \circ \alpha.$$

We denote by p, q, r the following quantities: $p = \frac{\partial w}{\partial x}$, $q = \frac{\partial w}{\partial y}$, and $r = \frac{\partial w}{\partial z}$. Starting from a result mentioned in [8], we admit that the trace of a propagating surface may be determined only by its normal velocity, as the other components of the velocity influence only the local parameterization. Our goal is then to compute the projected velocity of the evolving surface $F = \langle \pi \circ \alpha_t, \mathbf{n} \rangle$, $\mathbf{n} = (n_1, n_2, n_3)$ being the normal to the projected surface $\pi \circ \alpha(u, v, t)$. By using the same assumptions as in the bidimensional case, one can write the propagation of the projected surface $\mathcal{C}(t)$ along its normal by

$$\frac{\partial C}{\partial t} = F\mathbf{n}, \tag{8}$$

where the function F represents the propagation velocity of the surface along its normal. This velocity can be obtained by

$$F = \langle \mathbf{n}, \pi \circ \alpha_t \rangle,$$

where τ^u and τ^v are the tangential vectors of α defined by

$$\boldsymbol{\tau}^{\mathbf{u}} = \frac{\alpha_u}{\|\alpha_u\|} = \frac{(x_u, y_u, z_u, w_u)}{\sqrt{x_u^2 + y_u^2 + z_u^2 + w_u^2}} \qquad \text{and} \qquad \boldsymbol{\tau}^{\mathbf{v}} = \frac{\alpha_v}{\|\alpha_v\|} = \frac{(x_v, y_v, z_v, w_v)}{\sqrt{x_v^2 + y_v^2 + z_v^2 + w_v^2}},$$

and $\mathbf{N}$ the normal vector to W:

$$\mathbf{N} = \frac{*(W_x \wedge W_y \wedge W_z)}{\|*(W_x \wedge W_y \wedge W_z)\|} = \frac{(-p, -q, -r, 1)}{\sqrt{1 + p^2 + q^2 + r^2}}.$$

The propagation equation becomes

$$\alpha_t = \frac{1}{K} \times \begin{vmatrix} qz_u w_v - q w_u z_v - r y_u w_v + r y_v w_u + y_v z_u \\ -q z_u w_v + q w_u z_v + r y_u w_v + y_u z_v - r y_v w_u - y_v z_u \\ p y_u z_v - p y_v z_u - q x_u z_v + r x_u y_v + q x_v z_u - r x_v y_u \\ \text{additional term} \end{vmatrix}$$

with $K = \sqrt{1 + p^2 + q^2 + r^2}\sqrt{x_u^2 + y_u^2 + z_u^2}\sqrt{x_v^2 + y_v^2 + z_v^2}$.

Using the fact that the parameterization is orthogonal, one finds:

$$F = \langle \pi \circ \alpha_t, \mathbf{n} \rangle = \sqrt{a n_1^2 + b n_2^2 + c n_3^2 - d n_1 n_2 - e n_1 n_3 - f n_2 n_3} \tag{9}$$

with

$$a = \frac{1 + q^2 + r^2}{1 + p^2 + q^2 + r^2}, \qquad b = \frac{1 + p^2 + r^2}{1 + p^2 + q^2 + r^2}, \qquad c = \frac{1 + p^2 + q^2}{1 + p^2 + q^2 + r^2},$$

$$d = \frac{2pq}{1 + p^2 + q^2 + r^2}, \qquad e = \frac{2pr}{1 + p^2 + q^2 + r^2}, \qquad f = \frac{2qr}{1 + p^2 + q^2 + r^2}.$$

Having found the normal equation evolution of the projected surface, we now proceed to set up an Eulerian formulation for $\mathcal{S}(t)$, by writing that projected surface as a level-set $\varphi^{-1}(0)$. We derive such a formulation in the next section.

2.1.5. Level-set formulation. Given a function $\varphi : \mathbb{R}^3 \to \mathbb{R}$ such that its zero level-set tracks the projected surface $S(t) = \varphi^{-1}(0)$, one can determine that the function φ follows[2] the propagation equation

$$\frac{\partial \varphi}{\partial t} = \sqrt{a\frac{\partial \varphi^2}{\partial x} + b\frac{\partial \varphi^2}{\partial y} + c\frac{\partial \varphi^2}{\partial z} - d\frac{\partial \varphi}{\partial x}\frac{\partial \varphi}{\partial y} - e\frac{\partial \varphi}{\partial x}\frac{\partial \varphi}{\partial z} - f\frac{\partial \varphi}{\partial y}\frac{\partial \varphi}{\partial z}}, \tag{10}$$

the coefficients a, b, c, d, e, and f having the same values as in Eq. (9).

As mentioned in the curve evolution process described in [12] such as Eulerian formulation leads to numerical resolution schemes able to handle problems caused by a time varying coordinate system (u, v, t): curvature singularities and topological changes [17]. We describe, in the following section, the numerical resolution method used to solve Eq. (10). Then we use this numerical algorithm to build distance maps.

The numerical implementation is a generalization of the finite difference approximation described in [12, 14] for Hamilton–Jacobi type equations. It consists in an explicit temporal scheme where spatial derivatives are approximated by finite differences using the minmod function [14, 17, 18]. The derivative estimates can be bounded and the variations of the solution can therefore be controlled.

Using this numerical scheme, we can now use the computed function φ to generate distance maps on a manifold. In order to use Eq. (10) for computing the geodesic distance map of the surface discribed by a parameterization $\alpha(u, v, 0)$ on the 3-manifold W, we have to define an initial estimate φ_0 such that the initial surface is represented through a level-set of φ_0. This initial estimate can be obtained in several ways according to the data. We use a Euclidean distance map [2] in such a way that:

$$\varphi_0(x, y, z) = \begin{cases} -d(x, y, z) & \text{if } (x, y, z) \text{ is inside } \varphi_0^{-1}(0) \\ 0 & \text{if } (x, y, z) \in \varphi_0^{-1}(0) \\ +d(x, y, z) & \text{if } (x, y, z) \text{ is outside } \varphi_0^{-1}(0). \end{cases} \tag{11}$$

Given a graph hypersurface $X = W$ and the initial estimate $\varphi_0^{-1}(0)$ on this hypersurface, Eq. (10) characterizes the distance map of the area whose boundary is defined by $\varphi^{-1}(0)$.

2.2. Surface Matching

We can now use the previous theory to generalize the curve matching method presented in [5] to a matching process between two arbitrary surfaces $\mathcal{S}$ and $\mathcal{D}$ in $\mathbb{R}^3$. The two surfaces $\mathcal{S}$ and $\mathcal{D}$ are represented as 0-level-sets of two functions φ_0 and ψ_0. The two functions φ_0 and ψ_0 are computed from the initial data using the rule presented in (11). Then given these two initial functions φ_0 and ψ_0, the numerical process presented in Eq. (10) is used to generate two distance maps on the graph surface W: $D_{\mathcal{S}}$ and $D_{\mathcal{D}}$.

[2] It is important to note that the function φ depends not only on $(x, y, z) \in \mathbb{R}^3$, but also of the parameter t. To simplify the notations, we do not write explicity that dependence on t, but it is important to keep it in mind.

In this section we introduce the definition of the manifold W and how we use the distance maps to solve the surface matching. It is important to understand that the similarity criterion used in the matching process relies completely on the choice of W: each choice of W leads to a different matching result. In the following, we give an example for the definition of W.

2.2.1. Definition of a cost hypersurface modeling geometric properties. To take into account the geometrical properties of the surfaces to be matched, we use a graph hypersurface which takes into account the mean curvature of surfaces. This definition uses the curvature information in a small neighborhood of the source and destination areas. Within this neighborhood curvature information is relevant since only small deformation occurs and its curvature measure may be used to strengthen the matching of similar points. We characterize the local properties of the structures through the curvatures variation of the curves: $\Delta\kappa = \kappa_{\mathcal{S}} - \kappa_{\mathcal{D}}$, where $\kappa_{\mathcal{S}}$ and $\kappa_{\mathcal{D}}$ are respectively the mean curvatures of $\mathcal{S}$ and $\mathcal{D}$. In the case of small deformation we want the graph W to reflect the similarity between points having similar curvatures. This property will be down-weight as the distance increases. For that purpose, one can define ρ as

$$\rho(\Delta\kappa, d) = 1 - \frac{x^2}{1 + d^2x^2/\sigma}, \tag{12}$$

where σ is a scale parameter and d the Euclidean distance. The use of such a function to measure the similarity of the geometric properties allows reject or down-weight large dissimilarities. A set of robust error functions having the same behavior can be found in [15]. As the dissimilarities grow, the function ρ decreases and the function ρ approaches zero.

The graph hypersurface is then given by the following equation:

$$W = (x, y, z, \min(|\varphi_0|\rho(\Delta\kappa, |\varphi_0|), |\psi_0|\rho(\Delta_\kappa, |\psi_0|))). \tag{13}$$

$|\varphi_0|$ and $|\psi_0|$ are the Euclidean distance from respectively $\mathcal{S}$ and $\mathcal{D}$. The mean curvature is easily computed from the level-set representation of the surfaces:

$$\kappa = \frac{(\varphi_{yy} + \varphi_{zz})\varphi_x^2 + (\varphi_{xx} + \varphi_{zz})\varphi_y^2 + (\varphi_{xx} + \varphi_{yy})\varphi_z^2 - 2\varphi_x\varphi_y\varphi_{xy} - 2\varphi_x\varphi_z\varphi_{xz} - 2\varphi_y\varphi_z\varphi_{yz}}{\left(\varphi_x^2 + \varphi_y^2 + \varphi_z^2\right)^{3/2}}.$$

To smooth irregularities coming from real data or singularities in the graph W, we perform a gaussian convolution on the graphs W. This guarantees that the partial derivatives $\frac{\partial w}{\partial x}$, $\frac{\partial w}{\partial y}$, and $\frac{\partial w}{\partial z}$ are always defined.

2.2.2. Similarity measure and matching paths. Let $\mathcal{S}$ and $\mathcal{D}$ be two surfaces drawn on W and identified with "source" and "destination" surface. We want to compute minimal paths, on the manifold W, connecting $\mathcal{S}$ and $\mathcal{D}$. Wherever W is considered as a *cost hypersurface* such a path corresponds to paths of minimal cost between the two structures. Computing such a path amounts to searching for an optimal path among all the paths $p_{X_{\mathcal{S}}}$ starting at $X_{\mathcal{S}} \in \mathcal{S}$ and ending at a point $X_{\mathcal{D}} \in \mathcal{D}$ and minimizing a given cost function f. A cost function f can be easily derived using the fact, proven in [12], that the minimal path between $\mathcal{S}$ and $\mathcal{D}$ minimizes the sum of the distance maps. So we consider the cost function given

by

$$f(x, y, z) = \varphi(x, y, z) + \psi(x, y, z), \tag{14}$$

where φ and ψ are the bivariate functions defining the distance maps $D_{\mathcal{S}}$ and $D_{\mathcal{D}}$. Note that the function f may take negative values, as we take into account the interior and exterior of the surfaces. To define the matching paths we use a property of the graph surfaces $D_{\mathcal{S}}$ and $D_{\mathcal{D}}$ which relates the equal distance contour to minimal paths: the minimal paths are orthogonal to equal distance contours. Since the equal distance contours are level sets of the map $D_{\mathcal{S}} + D_{\mathcal{D}}$, a vector tangent to the matching path is defined by the gradient of the cost function:

$$\nabla f = \nabla\varphi + \nabla\psi.$$

This approach gives a reliable path construction scheme: given a point $X_{\mathcal{S}}$ on the source area, move this point in the opposite direction of the gradient of f until reaching a point on the destination area. The result is the minimal cost path connecting the two areas and starting at $X_{\mathcal{S}}$. This path $p(s)$ is defined by the parameterized curve $p(s)$ such that $p(0) = X_{\mathcal{S}}$, $p(1) = X_{\mathcal{D}}$ and

$$\frac{\partial p}{\partial s} = -\nabla(\varphi + \psi),$$

where $X_{\mathcal{S}} \in \varphi_0^{-1}(0)$ is given and $X_{\mathcal{D}} \in \psi_0^{-1}(0)$ is unknown. These orbits are obtained by applying a classical Runge–Kutta scheme.

2.3. Meteorological Result

Results displayed in the figures come from an experiment led on a Meteosat temporal sequence of an atmospheric depression in the tropics. The Meteosat satellite has a 30 minutes acquisition's frequency. In some situations, this temporal sampling is not sufficient to characterize the structures evolution and a model has to be considered. For example, in the tropics clouds structures aggregate and disaggregate rapidly. Figure 1 shows two frames of such a sequence. These frames come from a sequence provided by LMD (Laboratory of Meteorological Dynamics, Ecole Polytechnique, France), copyright (c) 2001 EUMETSAT. Data acquired in infrared channel measure the temperature. Regarding clouds

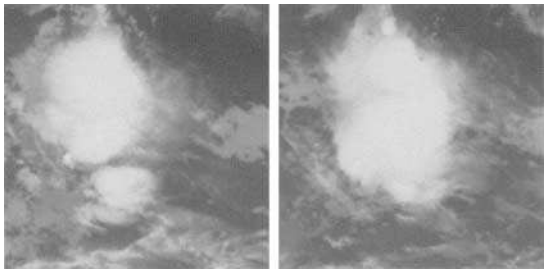

FIG. 1. Two consecutive images extracted from the same METEOSAT sequence.

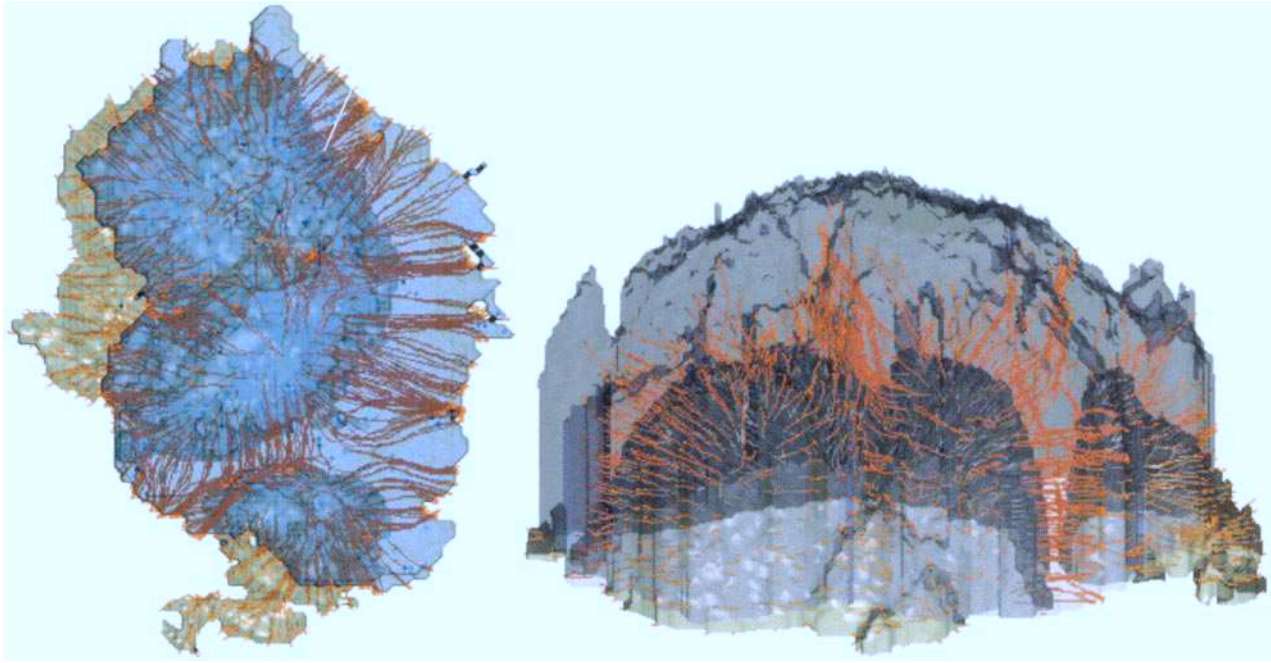

FIG. 2. Matching paths between the two meteorological structures.

observed on these data, it has been proved that cloud temperature is directly linked to the elevation hence leading to a measure of cloud elevation. This example is very interesting since the structure may deform rapidly and it displays large and small deformations at specific locations and changes of topology simultaneously. The matching is performed between the elevation maps of the two cloud structures extracted from Fig. 1. Figure 2 shows the result of the matching method. The leftmost cloud structure of Fig. 1 is clearly depicted with its two components. Above is the cloud structure corresponding to the elevation map of the rightmost image in Fig. 1. The matching paths are depicted in the two views of Fig. 2.

3. CONCLUSION

The research presented in this work introduces a new method for answering the problem of matching two objects. It relies on a geodesic distance evolution scheme written in the form of a partial differential equation for computing distance maps. The surface evolution scheme is a generalization of the geodesic curve evolution process presented in [12], leading to an algorithm for computing distance maps in 3-manifolds. The matching paths minimize a cost criterion which can incorporate various properties. The resulting matching algorithm allows us to take into consideration large deformations and topological changes between the source and destination surfaces. Use of the Hodge $*$ operator for deriving the surface propagation rule unveils a generalization of the matching process to any number of dimensions [10]. The level of generality of the matching process presented in this paper should give new insights to many problems in computer vision where the matching of complex structures is relevant.

REFERENCES

1. R. Abraham, J. E. Marsden, and T. S. Ratiu, *Manifolds, Tensor Analysis and Applications*, Springer-Verlag, Berlin/New York, 1988.
2. G. Borgefors, Distance transformations in arbitrary dimensions, *Comput. Vision Graphics Image Process* **27**, 1984, 321–345.
3. V. Caselles, R. Kimmel, and G. Sapiro, Geodesic avtive contours, *Internat. J. Comput. Vision* **22**, 1997, 61–79.
4. I. Cohen, N. Ayache, and P. Sulger, Tracking points on deformable objects using curvature information, in *ECCV*, Santa Margherita Ligure, Italy, May 1992, pp. 458–466.
5. I. Cohen and I. Herlin, Curves matching using geodesic paths, in *CVPR'98*, Santa Barbara, CA, June 1998, pp. 741–746, IEEE Comput. Soc. Press, Los Alamitos, CA.
6. U. R. Dhond and J. K. Aggarwal, Structure from stereo -a review, *IEEE Trans. SMC* **19**, 1989, 1489–1510.
7. M. P. do Carmo, *Differential Geometry of Curves and Surfaces*, Prentice-Hall, Englewood Cliffs, NJ, 1976.
8. C. L. Epstein and M. Gage, The curve shortening flow, in *Wave Motion: Theory, Modeling and Computation* (A. Chorin and A. Majda, Eds.), Springer-Verlag, New York, 1987.
9. J. Gomes and O. Faugeras, Level sets and distance functions, in *Proceedings of ECCV'2000*, Vol. 1, pp. 588–682, Dublin, Ireland, June/July 2000, IEEE Comput. Soc. Press, Los Alamitos, CA.
10. E. Huot, H. Yahia, I. Herlin, and I. Cohen, Surface matching with large deformations and arbitrary topology: a geodesic distance evolution scheme on a 3-manifold, in *Proceedings of European Conference on Computer Vision*, 2000.
11. M. Kass, A. Witkin, and D. Terzopoulos, Snakes: Active contour models, *Internat. J. Comput. Vision* **1**, 1988, 312–313.
12. R. Kimmel, A. Amir, and A. F. Bruckstein, Finding shortest paths on surfaces using levelset propagation, *IEEE Trans. Pattern Anal. Mach. Intell.* **17**, 1995, 635–640.
13. R. Malladi, J. A. Sethian, and B. C. Vemuri, Shape modelling with front propagation: A levelset approach, *IEEE Trans. Pattern Anal. Mach. Intell.* **17**, 1995, 158–175.

14. S. Osher and J. A. Sethian, Fronts propagating with curvature dependent speed: Algorithms based on Hamilton–Jacobi formulations, *J. Comput. Phys.* **79**, 1988, 12–49.
15. L. Robert and R. Deriche, Dense depth map reconstruction: A minimization and regularization approach which preserves discontinuities, in *Proceedings of the Fourth European Conference on Computer Vision 1996*, Vol. I, pp. 439–451, Cambridge, UK, April 1996.
16. B. Serra and M. Berthod, Optimal subpixel matching of contour chains and segments, in *ICCV*, pp. 402–407, Cambridge, MA, June 1995.
17. J. A. Sethian, *Level Set Methods: Evolving Interfaces in Geometry, Fluid Mechanics, Computer Vision and Materials Sciences*, Cambridge Univ. Press, Cambridge, MA, 1996.
18. J. A. Sethian and J. Strain, Crystal growth and dendritic solidification, *J. Comput. Phys.* **98**, 1992, 231–253.
19. M. Spivak, *A Comprehensive Introduction to Differential Geometry*, *Vol. I*, Publish or Perish, Berkeley, CA, 1971.
20. J. P. Thirion, Extremal points: definition and application to 3D image registration, in *CVPR*, pp. 587–592, IEEE Comput. Soc. Press, Los Alamitos, CA, 1994.
21. P. Thompson and A. W. Toga, A surface-based technique for warping 3-dimensional images of the brain, *IEEE Trans. Med. Imaging* **15**, 1996, 402–417.
22. T. Pajdla and L. Van Gool, Matching of 3D curves using semi differential invariants, in *ICCV*, pp. 390–395, Cambridge, MA, June 1995.
23. A. J. Van Doorn and J. J. Koenderink, Spatiotemporal integration in the detection of coherent motion, *Vision Res.* **24**, 1984, 47–53.
24. G. Xu and Z. Zhang, *Epipolar Geometry in Stereo, Motion, and Object Recognition: A Unified Approach*, Kluwer, Dordrecht Norwell, MA, 1996.
25. Z. Zhang and O. D. Faugeras, Estimation of displacements from two 3D frames obtained from stereo, *IEEE Trans. Pattern Anal. Mach. Intell.* **14**, 1992, 1141–1156.

ETIENNE HUOT is a senior researcher at the University of Versailles. He is involved in two laboratories: INRIA–Air Project and CNRS–CETP. The research of the Air Project is dedicated to image processing models applied to remote sensing data. On the other hand, the CETP laboratory's main purpose is to study environmental phenomena by using satellites. Hence, Etienne Huot's research relies on both model and thematic applications. His main research topic is the study of temporal evolution of earth phenomena by the use of deformable structures.

HUSSEIN YAHIA is a senior researcher at INRIA. His research interests are computers graphics, image processing and distributed information systems. His main topic of current research is the use of geometric models to analyze motion of deformable structures in satellite image sequences.

ISAAC COHEN is a research assistant professor in computer science. After five years as a researcher at the Institut National de Recherche en Informatique et Automatique (INRIA), he joined the Institute for Robotics and Intelligent Systems of USC in November 1997. His primary research interests are in variational methods for computer vision.

ISABELLE HERLIN is Director of Research at INRIA and the head of the Air project team. Her main research interests are: image processing of satellite sequences and integration of earth observation images together with processing models in environmental information systems.